SMA Memo #165

Science with the wideband Submillimeter Array: A Strategy for the Decade 2017–2027

ed. D. Wilner *contributing authors:* E. Keto, G. Bower, T.C. Ching, M. Gurwell, N. Hirano, G. Keating, S.P. Lai, N. Patel, G. Petitpas, C. Qi, TK Sridharan, Y. Urata, K. Young, Q. Zhang, J.-H. Zhao

Version 2.0, January 27, 2017

Figure 1: *The eight 6-meter antennas of the Submillimeter Array on Maunakea, Hawaii (photo by N. Patel).*

Contents

1 Executive Summary

The Submillimeter Array (SMA)[1] comprises eight movable 6-meter diameter antennas sited on Maunakea, Hawaii, designed for high spatial and spectral resolution observations at submillimeter wavelengths. Pioneering observations with the SMA have provided new insights into a wide variety of astrophysical phenomena, including the formation and evolution of galaxies, stars and planets, and the nature of the supermassive black hole at the center of the Milky Way. Following careful deliberation, the SMA project is embarking on an ambitious, staged, strategic upgrade that will increase its instantaneous bandwidth and dramatically improve its observational sensitivity and speed. The unique capabilities of this ultra-wideband SMA– the "wSMA"– promise to spark a new era of forefront discoveries.

In brief, the wSMA upgrade will provide a core receiver set providing dual-polarization observing bands covering the 345 GHz and 230 GHz atmospheric windows, each with 32 GHz of spectral coverage. Together with upgrades of the signal transport system and digital correlator, this brings a factor of 16 increase in instantaneous bandwidth from the original SMA capability. For continuum observations, speed increases linearly with bandwidth to a given level of sensitivity, enabling more observations to the same depth in the same amount of time. Or, for a given amount of time, the sensitivity increases as the square root of bandwidth, enabling deeper observations. For line observations, spectral coverage increases linearly with bandwidth, enabling observations of many lines simultaneously, all at high spectral resolution. In effect, every wSMA observation of an astronomical source is an imaging spectral line survey, and an enormous amount of information can be extracted from such data in conjunction with physical, chemical and dynamical models. This whitepaper elaborates on illustrative examples in key scientific areas, including the evolutionary state of protostellar sources, the chemistry of evolved star envelopes, the constituents of planetary atmospheres, starburst galaxies in the local Universe and at high redshifts, and even low-mass galaxies at high redshifts through the technique of intensity mapping. The wSMA speeds up observations to allow systematic, comparative studies of large numbers of spectral surveys for the first time. The wSMA also will be ideally suited for the study of sources in the time domain. Illustrative examples include the variability of the accretion flow onto the SgrA* black hole, capturing emission from gamma ray bursts from massive star deaths in the early universe and the mergers of compact objects that produce gravitational waves, and resolved spectroscopy of the pristine material that escapes from comets as they traverse the inner Solar System.

The wSMA will be complementary to the larger international Atacama Large Millimeter/ submillimeter Array (ALMA) in Chile, which followed the SMA into submillimeter interferometry in 2011. The immense time pressure on ALMA from its many constituencies only creates an increasing need for the wSMA, notably for the large class of observations that do not require ALMA's full sensitivity or angular resolution, as well as for unique submillimeter access to the northern sky. The wSMA will play a leading role in select science areas in the ALMA era, including those requiring long-term programs to build large samples, or rapid response based on flexible scheduling, as well as for high risk seed studies specifically designed for subsequent ALMA follow-up. In addition, the wSMA will be a critical station for submillimeter VLBI observations of supermassive black holes in the global Event Horizon Telescope, which will be bolstered by the inclusion of ALMA in 2017. Finally, the wSMA design explicitly incorporates open space for additional instrumentation to pursue new and compelling science goals and technical innovations, continuing its role as a pathfinder for submillimeter astronomy.

[1]The Submillimeter Array is a joint project between the Smithsonian Astrophysical Observatory and the Academia Sinica Institute of Astronomy and Astrophysics and is funded by the Smithsonian Institution and the Academia Sinica.

2 The Submillimeter Array in the ALMA Era

The Submillimeter Array (SMA), a collaborative project of the Smithsonian Astrophysical Observatory (SAO) and the Institute of Astronomy and Astrophysics of the Academia Sinica (ASIAA), was conceived as an exploratory telescope for high resolution observations at submillimeter wavelengths, between the radio bands where many other telescopes operate and far-infrared wavelengths accessible only from airplane altitudes or space. The SMA consists of eight 6-meter antennas sited on Maunakea, Hawaii, that operate together as an interferometer. With maximum baselines of 500 meters, the SMA was the first observatory capable of submillimeter wavelength imaging and spectroscopy at subarcsecond resolution. The SMA is also a pioneer in the development of instrumentation for submillimeter radio astronomy, particularly in the area of wideband receivers and electronics.

The SMA, in continuous operation since 2004, has made advances in many areas of astrophysics. In general, submillimeter observations are sensitive to cool matter at 10-100 K that is key to understanding the formation of planets, stars, and galaxies across cosmic time. Other important applications include studies of synchrotron emission from dense plasmas, which become partly transparent at submillimeter wavelengths. Astronomers have published more than 700 refereed papers using SMA data that collectively have garnered more than 21,000 citations. Selected science highlights include

- Imaging a newly discovered population of submillimeter-bright, strongly gravitationally lensed galaxies at high redshits with intense star formation, probing the growth of the most massive galaxies (Negrello et al., 2010; Cañameras et al., 2015).
- Spatially mapping bolometric luminosity in ultraluminous galaxies to distinguish deeply obscured heating sources as starbursts or black holes (Sakamoto et al., 2008, 2013).
- Using dust polarization observations to reveal directly where magnetic support is overcome by gravity in the dense cores where Sun-like stars form (Girart et al., 2006) and in high-mass star forming regions (Zhang et al., 2014).
- Characterizing planet-forming disks around young stars on the size scales of Solar Systems (Andrews et al., 2009), including discovery of inner cavities that point to the presence of emerging planetary systems (Andrews et al., 2011).
- Producing a resolved chemical inventory of an evolved star envelope that isolated the stellar wind acceleration zone (Patel et al., 2011) and aided identification of new molecules in space (Cernicharo et al., 2015).
- Using the SMA as a critical station in millimeter VLBI experiments to detect event-horizon-scale structure around supermassive black hole candidates in our Galactic Center and in M87 (Doeleman et al., 2008, 2012; Johnson et al., 2015).

The international Atacama Large Millimeter/submillimeter Array (ALMA) in Chile recently became capable of submillimeter interferometry, with early science operations starting in 2011. ALMA has larger collecting area and more comprehensive baseline coverage than the SMA, and it is possible to configure ALMA to make equivalent observations to the SMA at much faster speed. However, the high time pressure on ALMA does not allow it to make all important observations, and ALMA by itself cannot provide a complete view of the submillimeter universe. As a result, competition to use the SMA remains fierce in the ALMA era, with 3:1 oversubscription for submillimeter observing time. For longer millimeter wavelengths that overlap with ALMA, the IRAM NOrthern Extended Millimeter Array (NOEMA) in France is undergoing a dramatic expansion to double its collecting area. The SMA, with carefully considered upgrades, will remain an essential resource for forefront

submillimeter studies, in particular for observations of the large class of objects that do not require the full resolution or sensitivity of ALMA, for focused large scale programs aimed at statistically significant samples, for curiosity driven and high risk ideas, and for unique submillimeter access to the northern sky. The SMA also plays a key role in submillimeter VLBI observations as part of the global Event Horizon Telescope, which will include ALMA as a station for the first time in 2017.

The modest scale of the SMA allows for rapid adoption of technical innovations and nimble scheduling of science observations, two basic properties that will keep the telescope competitive and exciting going forward. Following the recommendations of a detailed study by the *2010 SMA Futures Committee* (Fazio et al., 2010), reaffirmed by the *2014 SMA Visiting Committee* (Harris et al., 2014), the SMA project is embarking on an ambitious, staged, strategic upgrade to increase the power of the telescope by expanding its instantaneous bandwidth while simultaneously maintaining high spectral resolution. The full increase is a factor of 16, from the original 8 GHz (= 2 GHz × 2 sidebands × 2 receiver bands) to 128 GHz (= 16 GHz × 2 sidebands × 2 polarizations × 2 receiver bands). In §3, we describe briefly this upgraded, ultra-wideband SMA– the "wSMA". In §4, we outline important science applications enabled by its unprecedented capabilities.

3 Ultra-wideband Performance Improvements

The wSMA offers a new "core" receiver set providing two dual-polarization observing bands with LO ranges 280–360 GHz and 210–270 GHz, each with an IF band that spans 4–20 GHz. (Selection hardware will also allow a separate receiver to operate alongside the core receiver, see §5.2.) These wideband receivers are enabled by the series connected, distributed SIS mixer concept demonstrated by Tong et al. (2005) and fabricated by ASIAA (Figure 2). The correlator will process 128 GHz total bandwidth, all at high spectral resolution ($\lambda/\Delta\lambda \sim 2.5 \times 10^6$). This digital back end capability relies on open-source signal processing technology developed by the Collaboration for Astronomy Signal Processing and Electronics Research (CASPER, Parsons et al. (2009)). This combination of wide bandwidth with simultaneous, uniform spectral resolution, and subarcsecond angular resolution, is unparalleled at submillimeter wavelengths. As Figure 3 shows, this unique capability will provide for dual receiver, dual polarization operation, enabling simultaneous observations in the two atmospheric windows that are typically wide open from the Maunakea site, each with 32 GHz of spectral coverage.

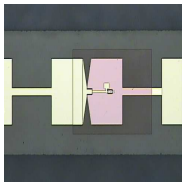

Figure 2: *SMA 345 band mixer chip fabricated by ASIAA.*

	year	receiver bandwidth	bands × pols	total bandwidth	number of channels	continuum rms (μJy) 230 GHz	345 GHz
stage 0	2004	2 GHz × 2 sb	2	8 GHz	1.2288×10^4	600	1250
stage 1	2016	8 GHz × 2 sb	2	32 GHz	5.24288×10^5	230	520
stage 2	2020	16 GHz × 2 sb	4	128 GHz	2.097152×10^6	140	330

Table 1: *Timeline of the SMA bandwidth expansion. The fully upgraded receivers, IF hardware, and digital correlator will enable observations spanning 16 GHz in each of 2 sidebands and 2 polarizations, in the 230 and 345 GHz atmospheric windows simultaneously. The maximum number of channels listed is for each baseline. The continuum rms noise values correspond to a full 10 hour track (2/3 on-source) for a target at +30° declination above 20 degrees elevation, with 1 mm pwv at 345 GHz and 2 mm pwv at 230 GHz. These tabulated values also incorporate receiver improvements.*

The implementation plan for the wSMA upgrade has been staged carefully. By the end of 2016, 1/4 of the new technologies will be installed and available to astronomers, using the existing infrastructure. Figure 4 provides an example of the spectral coverage available, spanning 16 GHz on the

sky, all with 140 kHz channels. The full wSMA capability will follow with the completion of new cryostats for the core receivers, and further build out of the digital backend. Table 1 summarizes the timeline and capabilities of the bandwidth expansion. For continuum, the characteristic rms sensitivity for a full track will be 330 μJy at 345 GHz and 140 μJy at 230 GHz. For lines, the rms brightness temperature in a 0.″75 synthesized beam will be 1.0 K in 1 km s^{-1} in both receiver bands. The expanded bandwidth improves the performance of the telescope by increasing its instantaneous sensitivity and observing speed. The improvement is described differently depending on the observing mode, as described below.

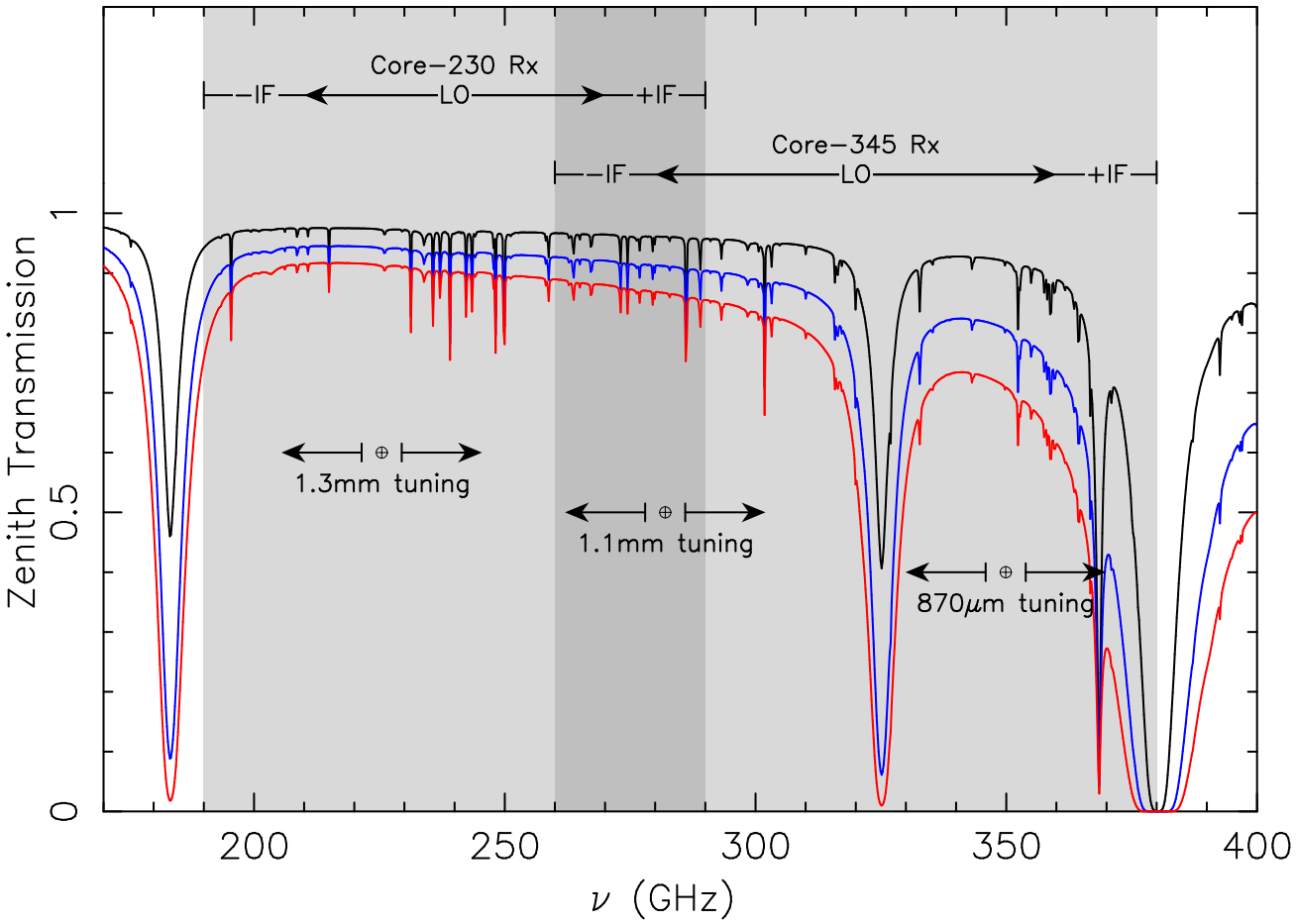

Figure 3: *Schematic spectral coverage of the ultra-wideband SMA, showing the full tuning ranges across the 230 and 345 GHz atmospheric windows. Lines show atmospheric transmission for the best weather conditions, top quarter, and top half of the time. Also shown are examples of the instantaneous spectral coverage near 1.3 mm (230 GHz), 1.1 mm (270 GHz), and 0.87 mm (350 GHz).*

3.1 Continuum: Sensitivity, Imaging, and Angular Resolution

For observations of continuum emission, the signal power received by the telescope is proportional to the bandwidth. To a given level of sensitivity, the observing speed increases linearly with the bandwidth. The wSMA, with 16 times the bandwidth of the original SMA, can make 16 times as many observations to the same sensitivity. Alternatively, within a given amount of time, the sensitivity increases as the square root of the bandwidth.

The expanded bandwidth improves not only the speed and sensitivity of the telescope but it also improves the ability to make images. The fidelity of wideband continuum images may be dramatically improved using the technique of multi-frequency synthesis. Also, more sources become amenable to imaging at higher angular resolution. The SMA can make observations at different

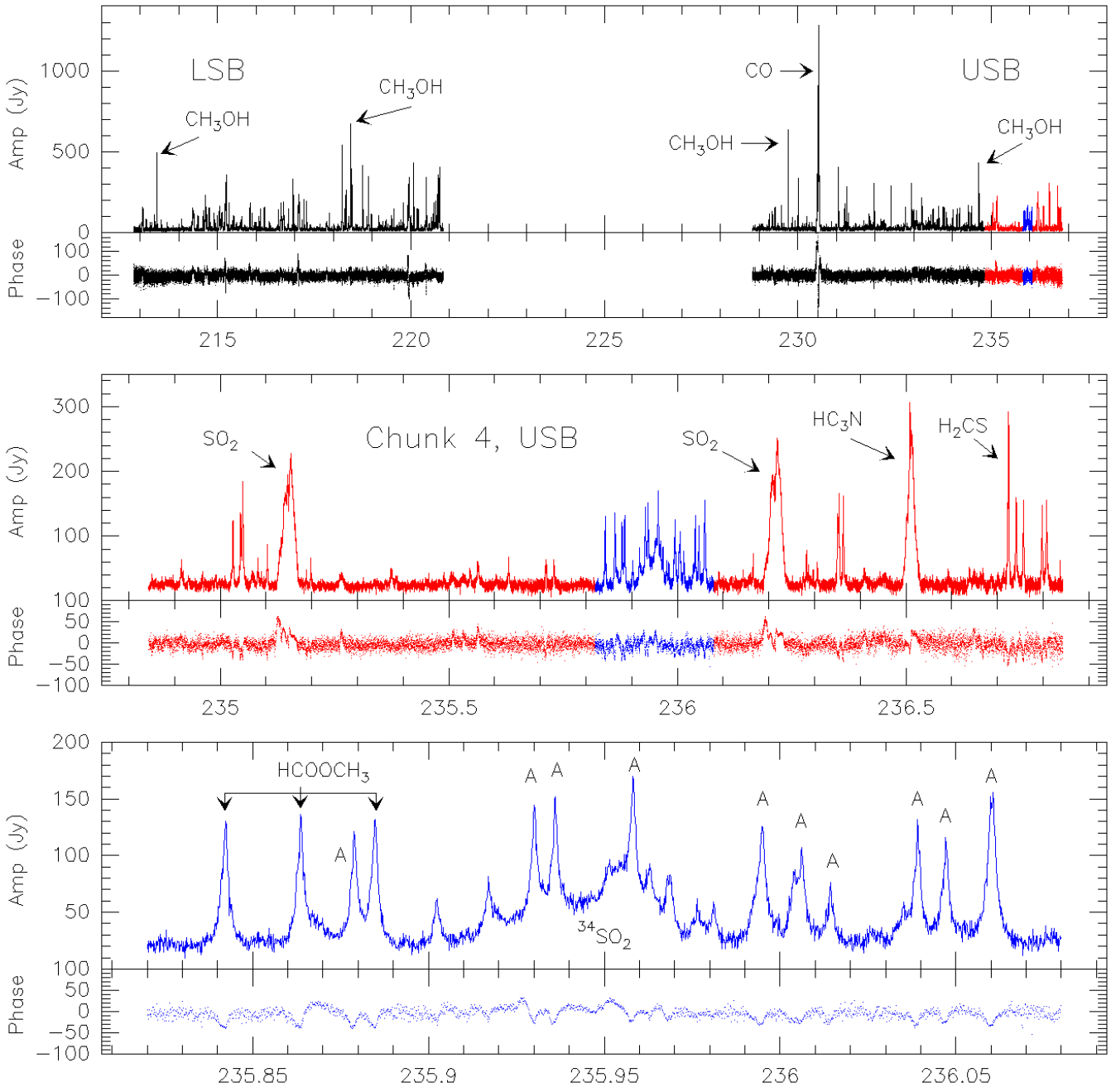

Figure 4: *Example of an SMA single baseline spectrum of the Orion-KL region using SWARM with instaneous spectral coverage of 8 GHz per sideband, at 140 kHz resolution, from Primani et al. (2016). The middle and lower panels present increasingly zoomed views of small sections of the spectrum above them (indicated in red and blue). A multitude of highly structured and resolved spectral line features in amplitude and phase are identified from a variety of molecular species ("A" indicates* $^{13}CH_3OH$*).*

angular resolutions by relocating the individual antennas. Often, the choice of resolution for an interferometer is limited by the available sensitivity. If an astronomical source is extended enough to be resolved, the area of the source seen by the telescope beam (and therefore the power received by the telescope) decreases with increasing angular resolution. Therefore, more sensitivity is required to achieve higher resolution. While the expanded bandwidth does not increase the maximum resolution

of the telescope, the increased power received by the expanded bandwidth allows a source of a given brightness to be observed at higher angular resolution, up to the maximum resolution of the telescope.

3.2 Lines: More Spectral Coverage, Faster Surveys

For observations of spectral lines, the expanded bandwidth allows for simultaneous observations of a larger part of the spectrum, and thus faster coverage of more lines. In this mode, the spectral coverage increases linearly with the bandwidth. Most spectral line observations made with the SMA seek to take advantage of the large number of spectral diagnostics in the submillimeter spectrum, including rotational transitions of many molecules and atomic fine structure lines. As a result of the upgrade, full suites of spectral lines can be obtained in a single observation, with no need for multiple observations to scan across the spectrum.

3.3 Improved Calibration

All observing modes are improved by more accurate calibration made possible by the increased sensitivity from the expanded bandwidth. Fluctuations in the Earth's atmosphere cause variations in the signal received from an astronomical target, and interferometers like the SMA track these variations by periodically observing a calibrator source, typically a point-like quasar, interleaved with observations of the astronomical target. The improvement in instantaneous continuum sensitivity from an expanded bandwidth allows the use of fainter quasars, and significantly improves the chances of finding a suitable calibrator close to the astronomical source. This improves the accuracy and speed of calibration. In addition, more targets will have high enough signal-to-noise ratios on short timescales to use "self-calibration" techniques to improve temporal gain calibration and achieve better image fidelity and higher dynamic range.

3.4 Operations and Data Archive

The new instrumentation will be operated and maintained by the regular staff of the SMA telescope, consisting of about 35 technical staff and researchers located in Hilo, HI, Cambridge, MA and Taipei, Taiwan. The telescope operations will be significantly simplified by the ultra-wideband capability. A very limited number of standardized receiver setups will satisfy the requirements of most science observations, which will reduce the time devoted to receiver setup and also save on calibration overheads. Moreover, the digital correlator has only a single configuration that provides high spectral resolution over the full bandwidth at all times, thereby eliminating the need to support multiple modes and setups. The archived data rate will increase in proportion to the bandwidth, to typically 0.2 Tb/night, an amount that is already easily accommodated by current storage technology. Together, the standardization and simplification of receiver and correlator setups will combine to make for a highly homogeneous data archive, which will be comparatively easy for users to mine.

3.5 The ALMA Context

While there are no wSMA observations that are beyond the means of ALMA in principle (outside of the northern sky), there are key applications that capitalize on the strengths of the unique, instantaneous wide bandwidth of the wSMA.

The main array of ALMA, with fifty 12 meter antennas, has 25× larger collecting area than the wSMA, but using ALMA for spectral scans is particularly inefficient, especially for wide fields that require mosaicking. The wSMA, with 8× wider bandwidth, $\sim$ 4× higher spectral resolution (for wide bandwidths), and 4× larger field of view, approaches the ALMA main array capabilities in this

regime (and in fact exceeds it for bright objects after accounting for the current overheads). The wSMA will be more capable in many ways than the "ALMA Compact Array" (ACA) comprised of twelve 7 meter antennas, as wider bandwidth more than makes up for 2× smaller collecting area. ALMA, in recognition of the intrinsic value of observations with the ACA alone, opened this mode for proposals in Cycle 4, and plans to maintain its availability.

The wSMA can easily devote weeks or months of observing time to individual programs; ALMA is unlikely to commit to such large allocations in the forseeable future, given the many constituencies it must serve. Such long-term programs allow for the build-up of very large samples, and extensive time monitoring. Another important aspect is that the more nimble wSMA can respond within minutes to targets of opportunity, and potentially even faster, as well as provide rapid follow-up to discoveries made with other telescopes (including ALMA), between the ALMA annual proposal cycles.

Astronomical research rarely relies on the data from one telescope alone and is best served by access to different facilities with both complementary and unique capabilities. Observations from one telescope can be readily followed up elsewhere at a different wavelength or resolution. We can expect strong synergies between the wSMA and ALMA, despite the difference in scale. The situation is analogous to the very successful cooperation of optical telescopes with a wide range of sizes, e.g. SAO's Whipple Observatory on Mt. Hopkins with its suite of 1.3, 1.5 and 6.5 meter telescopes, or the university scale high performance computer clusters, like Harvard's Odyssey cluster, and much more powerful supercomputers at U.S. national facilities like those at NCSA or Oak Ridge. Recall that some of the most significant and unexpected discoveries in astrophysics in recent years were obtained with very modest telescopes, not the largest ones available.

4 Ultra-wideband Science Examples

The SMA is engaged in a wide variety of astronomical observations, all of which benefit from the increased sensitivity and speed provided by the wSMA expanded bandwidth. The following sections provide several illustrative examples; these are not meant to be a comprehensive list.

4.1 Spectral Line Surveys

With the wSMA, every observation of an astronomical source will be an imaging spectral line survey. The number of molecular lines within a given spectral bandwidth generally increases at shorter wavelengths, and observations in the submillimeter cover an abundance of lines compared to those at longer radio wavelengths. The brightness of these lines contains information on abundances of the species along with temperatures and densities, and the shapes of the lines encode information on the gas motions. An enormous amount of information can be extracted from spectral line observations when used in conjunction with physical, chemical and dynamical models.

The SMA has engaged in a number of wide bandwidth spectral line surveys, including low-mass and high-mass star forming regions (Jørgensen et al., 2011; Cyganowski et al., 2014), evolved asymptotic giant branch stars (Patel et al., 2011; Kamiński et al., 2013), and starburst galaxies (Martín et al., 2011). The amount of spectrum and the number of distinct molecular lines that can be observed at one time is directly proportional to bandwidth. The wSMA will significantly speed up such observations, such that it becomes feasible to compare in detail spectral line surveys from multiple sources within a given class of astrophysical object.

4.1.1 Star Forming Regions

Spectral line surveys of molecular cloud cores in the Galaxy seek to characterize the physical and chemical conditions that lead to the formation of stars and star clusters. Since molecular hydrogen– the main mass constituent– is not excited in the cold, dense concentrations where stars form, essentially all of our knowledge of the early stages comes from the radiation of trace constituents that emerges from the dark, dusty cores to reveal the structures within.

The quality and quantity of data on star forming regions is growing rapidly. Extensive continuum surveys performed by dedicated programs with single-dish telescopes provide complete samples of thousands of dense cores involved in star formation, both for the nearest clouds to the Sun and throughout the inner Galaxy. A major goal is to exploit the complexity of interstellar chemistry to probe the evolutionary state of these cores, which have masses in the range 1 to 1000 $M_\odot$. Rather than continuing to observe only the brightest or most easily accessible spectral lines, the next step will be comprehensive multiline studies, using high enough angular resolution to separate the important centers of activity.

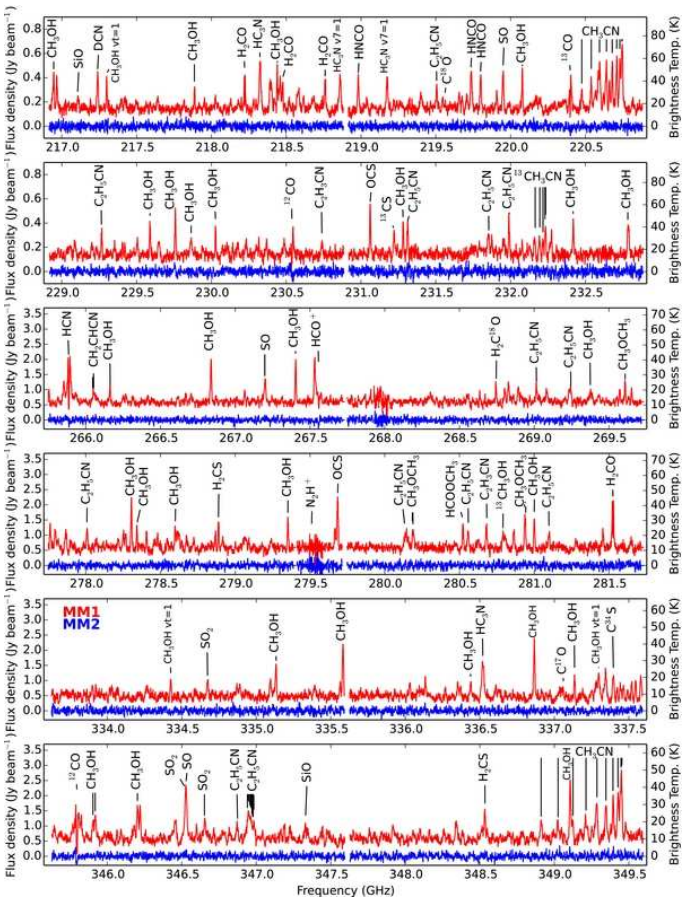

Figure 5: *SMA spectra covering 24 GHz towards two dust continuum peaks in the G11.92-0.61 star forming region, MM1 (red) and MM2 (blue), which are separated by only* $\sim$ 0.12 *pc. The rich spectrum of MM1 indicates a protostellar hot core, while paucity of spectral lines in MM2 suggests it is starless. (Cyganowski et al., 2014)*

Figure 5 shows a slice of the submillimeter spectrum from two dust continuum peaks in a typical massive star-forming region, separated by only $\sim$ 0.12 pc but apparently at very different stages of evolutionary development (Cyganowski et al., 2014). Around the youngest source, MM2, there are very few spectral lines. At very cold temperatures, many molecules are frozen onto dust grains and their gas phase abundance is low. As a protostar grows in mass and luminosity and heats its surroundings, molecules come off the dust grains and are excited by collisions to radiate in the submillimeter. Powerful bipolar jets from the forming stars create localized shocks that also change the chemistry. The spectra in Figure 5 cover 24 GHz bandwidth, obtained in 3 different tunings with 2 receivers. The wSMA will provide data covering more than twice this bandwidth in a single observation in two polarizations, thereby accessing a rich set of chemical species in much shorter time. Progress in finding the most useful combinations of molecular probes likely will be empirical, and we are only just at the threshold of achieving any success in this endeavor. The wSMA will enable systematic, comparative molecular line studies of large samples.

Similar considerations apply to star formation processes on galactic scales. Spectral line surveys of nearby starburst galaxies probe the conditions that lead to the formation of super star clusters. These massive clusters, found in all starburst environments, may be the basic building blocks of star formation across cosmic time, as well as the precursors to the present day analogues of globular

clusters. (A prime target for the wSMA is M82, the prototype starburst galaxy, located in the northern sky and not accessible to ALMA.)

Spectral surveys also contain the chemical fingerprints associated with the dominant heating mechanisms in the nuclear regions of galaxies, distinguishing starbursts from the higher energy input of deeply embedded supermassive black holes. As an example, Figure 6 shows an SMA line survey of the double nucleus of the ultraluminous galaxy Arp 220, covering 40 GHz (30% of the 230 GHz atmospheric window) (Martín et al., 2011). This first aperture synthesis unbiased spectral line survey toward an extragalactic object required 10 separate tunings over 5 nights, and would be dramatically superceded by the wSMA in both spectral coverage and sensitivity with a comparable investment of time. At least 80% of the observed band is filled with molecular emission, with 73 features identified from 15 molecular species and 6 isotopologues. Taken as a whole, the chemistry is indicative of a purely starburst heated interstellar medium and shows no clear evidence of the influence of a black hole. In particular, an overabundance of H_2S and the low isotopic ratios observed are evidence of an environment chemically enriched by consecutive bursts of star formation, with an ongoing burst at an early evolutionary stage. The high abundance of water ($\sim 10^{-5}$) derived from the isotopologue $H_2^{18}O$, as well as vibrationally excited emission from HC_3N and CH_3CN provide evidence of high-mass star forming regions. Moreover, these observations put strong constraints on the compactness of the starburst event in Arp 220, requiring several million hot cores like the SgrB2 region in our Galactic Center concentrated within 700 pc.

4.1.2 High Redshift Galaxies

Intense star formation heats interstellar gas to typical temperatures of a few hundred K. This gas emits primarily in the infrared, but this radiation is red-shifted to the submillimeter when emitted by sources in the early Universe. Thus submillimeter wavelengths are ideal, and essential, for studying star and galaxy formation across cosmic time. Single dish submillimeter telescopes can search large areas of the sky for distant submillimeter emission. The prodigiously star-forming, high-redshift population of "Submillimeter Galaxies" is especially interesting, since these objects are typically very faint or undetectable in the optical but become readily detectable in the submillimeter with flux densities of a few mJy at 345 GHz, corresponding to total far-infrared luminosities of $> 10^{13}$ $L_\odot$. Surveys with Herschel and Planck have allowed rapid advances in the statistical knowledge of this population, albeit at angular resolutions too coarse to study the individual galaxies in much detail. The SMA has helped characterize this population not only by providing accurate positions to identify the submillimeter emission with particular optical or infrared counterparts, if present, for follow-up (Younger et al., 2007, 2009; Dowell et al., 2014), but also by determining the fraction of multiple or lensed systems (Negrello et al., 2010; Wang et al., 2011; Bussmann et al., 2013; Cañameras et al., 2015). In cases where gravitational lensing provides magnification, the effective sensitivity is boosted; thousands of such lenses are known across the sky. The spatial structure of the continuum enables modeling of the lensing and intrinsic brightness, and thus the morphology and star formation rate of the high redshift galaxy.

The increased sensitivity of the wSMA will speed continuum imaging and allow for both studies of fainter populations of distant galaxies, and for dramatic increases in the sample sizes of the brighter (and especially lensed) targets. But, the impact of ultra-wideband capabilities on spectroscopy will be revolutionary. The left panel of Figure 7 shows a spectrum of a lensed galaxy at z=3.91 made with a grating spectrometer (Zspec) on the single-dish Caltech Submillimeter Observatory that covers the full 230 GHz atmospheric window, showing multiple redshifted CO and H_2O rotational lines and N^+ (Bradford et al., 2011). The expanded bandwidth of the wSMA will enable rapid spectral coverage of distant galaxies like this, while imaging with more than 100× higher spectral resolution. The right panel of Figure 7 shows the line profile of C^+ in the z=5.24 lensed galaxy HLSJ091828.6+514223

from SMA observations (Rawle et al., 2014), which is spatially and spectrally resolved into at least four distinct kinematic components, interpreted as two interacting galaxies and an outflow. The wSMA will enable the transition from observations of a single line to observations of suites of lines, including fine structure lines of atomic and ionized C, N, and O (even with only a crude estimate of the redshift from photometric methods). At any redshift, there will be two or three CO lines available for detection, enough to allow an accurate determination of the redshift without any prior information.

The combination of the continuum, molecular lines, and atomic fine structure lines allows for characterization of primordial starbursts. The fine structure lines derive mainly from the neutral hydrogen phase of the interstellar medium, where the gas has been warmed by ultraviolet radiation from massive stars. The ratio of the C or CII to the infrared continuum (observed in the submillimeter) is inversely proportional to the strength of the ultraviolet radiation. This ratio and the continuum together measure the beam filling factor and the size of the starburst. Because atomic O is significantly excited only above 100 K, the ratio of atomic O to C or CII indicates the temperature of the neutral gas. The CO lines measure the column density of the molecular gas. These are the key parameters needed to investigate star formation evolution.

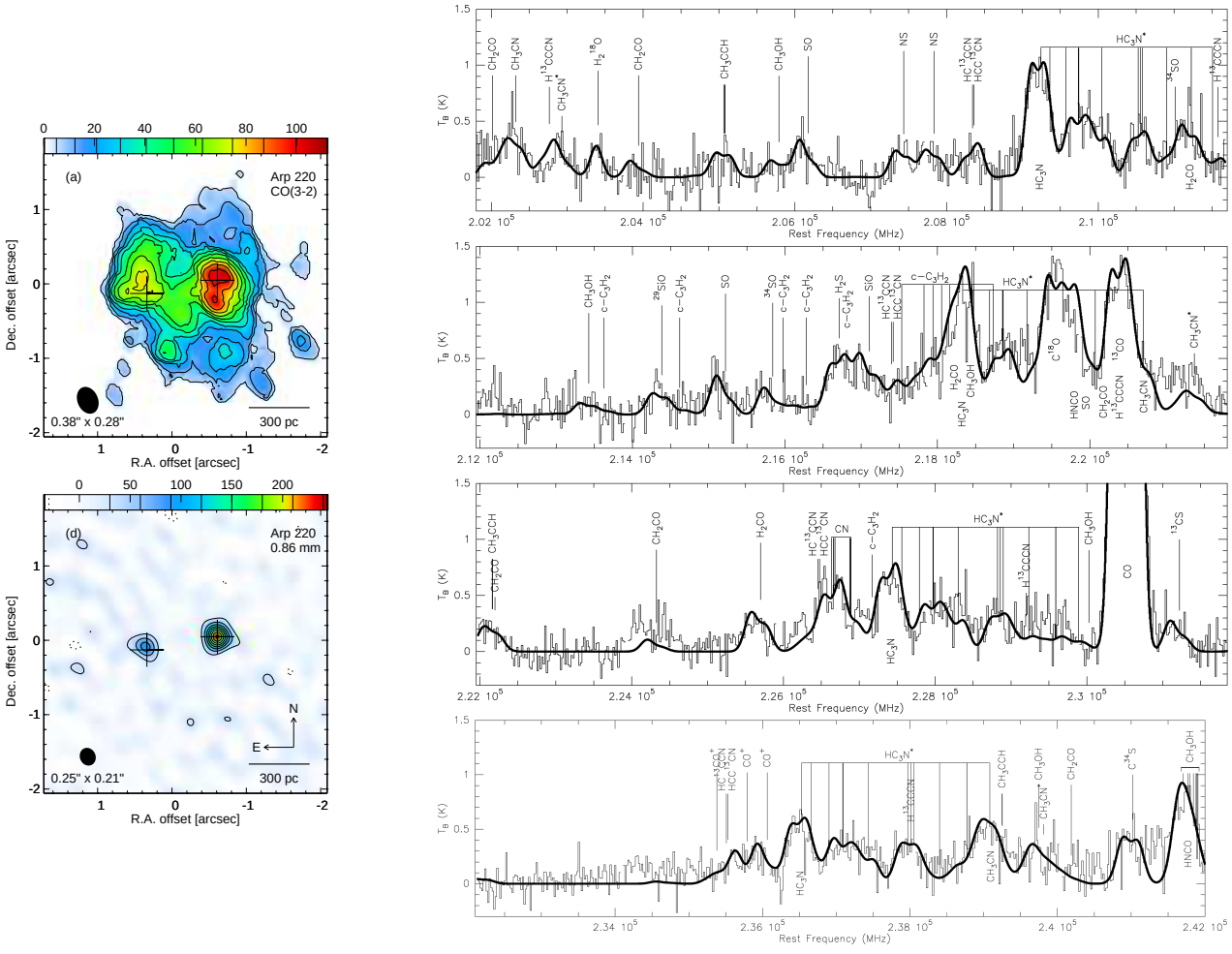

Figure 6: (left) *SMA subarcsecond images of CO 3-2 line and dust continuum emission of the nearby ultraluminious galaxy Arp 220, from Sakamoto et al. (2008).* (right) *The composite SMA 1.3 mm spectral scan of the nuclear region of Arp 220, from 202 to 242 GHz (Martín et al., 2011). The thick solid curve shows an LTE model of the identified molecular species, consisting of two kinematic components (one for each of the nuclei visible in the images).*

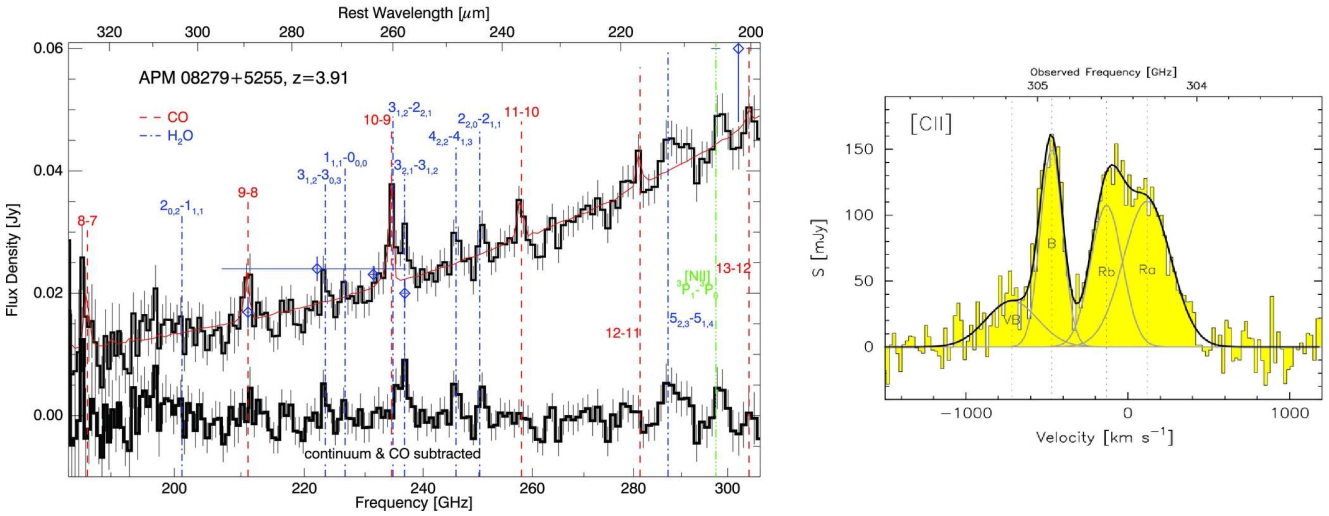

Figure 7: (left) *A Zspec grating spectrum of the z=3.91 lensed galaxy APM 08279+5255, showing multiple lines of CO, H_2O, and N^+ (Bradford et al., 2011). The wSMA will be capable of surveying systems like this at* 100× *higher spectral resolution, allowing precise spectroscopic redshift determinations (even when only crude SED-based model fits are available), and at the same time obtaining high resolution studies of morphology.* (right) *Integrated line profile of C^+ in the z=5.24 lensed galaxy HLSJ091828.6+514223, spectrally resolving at least four distinct kinematic components in this system (Rawle et al., 2014).*

4.1.3 CII Intensity Mapping

While sensitive observations with the wSMA, as well as ALMA, VLA and NOEMA make it possible to probe cool ISM of massive galaxies out to redshifts aproaching $z \sim 7$ (e.g. Riechers et al., 2013; Maiolino et al., 2015), the extraordinary objects detected are not likely to be characteristic of the overall population of star-forming galaxies in the early Universe, made up primarily of smaller and less luminous systems (Smit et al., 2012). Unfortunately, the line emission arising from the molecular gas of normal (low-mass) star-forming galaxies at high redshift is extremely faint. Direct detection of individual high-redshift galaxies is an expensive observational proposition, even with ALMA (which was explicitly designed to detect CO from a Milky Way analog at high redshift in 24 hours). The individual detection of a sufficient number of normal, high-redshift galaxies (i.e., hundreds or thousands of such objects) to properly characterize the underlying population is beyond the present generation of radio and submillimeter facilities (Keating et al., 2015).

An alternate method for exploring the molecular gas contents of early galaxies is the technique of "intensity mapping", where the emission from thousands or millions of galaxies is detected as large-scale fluctuations in mean line intensity. Intensity mapping has been the subject of numerous theoretical and observational studies, demonstrating it to be an effective and efficient method for performing blind surveys over large volumes– millions of cubic megaparsecs. The wSMA, with its larger field-of-view than other submillimeter interferometers, compact array configurations, and ultrawide bandwidth, is ideally suited to intensity mapping experiments. Moreover, while the signal of interest is expected to be unpolarized, the dual-polarization receivers of the wSMA allow for improved control of systematics and exploration of contaminants in the measurement.

In the local Universe, CO is used as the tracer of choice for studying the bulk of molecular gas in galaxies. However, galaxies in the early Universe may not possess enough dust to shield CO from the dissociating ultraviolet starlight, creating "CO-dark" molecular clouds (Wolfire et al., 2010). But this lack of dust may also lead to an increase in CII line emission. CII line emission typically traces the cool and neutral components of the ISM, with some arising from the photon-dominated regions surrounding molecular clouds. However, theoretical models also suggest that a lack of dust may

significantly enhance CII emission in molecular gas, making it a good tool for studying molecular gas at high redshift (Narayanan & Krumholz, 2016).

The frequency coverage of the wSMA allows for intensity mapping experiments targeting CII emission between $z = 3.5$ to 10, enabling exploration of the broad population of galaxies during the Epoch of Reionization ($z \sim 6$ to 10) and in the lead-up to the peak of cosmic star formation. As intensity mapping experiments generally require very large volumes to be surveyed, very wide bandwidths that sample larger instantaneous volumes allow for significantly improved sensitivity, affording the opportunity to study the evolution of the CII signal with redshift.

While theoretical models suggest that the wSMA is sensitive enough to detect an aggregate CII signal, CII intensity mapping experiments focused on $z \sim 6$ to 10 are also likely to face challenges due to line confusion, where interloper CO rotational line emission from lower-redshift galaxies may act as a contaminant (Breysse et al., 2015). Fortunately, with its wide bandwidth, the wSMA will be well suited for cross-correlation analysis between different CO rotational transitions. Such analysis will not only be valuable in eliminating line confusion, but it will allow the exploration of molecular gas through the higher rotational transitions of CO for galaxies at $z \gtrsim 1$ (Lidz & Taylor, 2016).

4.1.4 Evolved Stars

Low to intermediate mass (1-8 $M_\odot$) mass stars produce most of the carbon, nitrogen, and oxygen in the Universe, as well as most of the less common, lighter S-process elements. Forged in the thermonuclear furnace of the stellar interior, these elements are released when a dying star sheds its outer layers in a massive outflowing wind. In the Asymptotic Giant Branch (AGB) phase of evolution, the stellar envelopes of these stars have relatively low temperatures ($\sim$2000K), allowing the formation of simple molecules and even solid particles. Radiation pressure expels these particles out of the envelope, dragging the gas along with them, with mass-loss rates as high as 10^{-5} $M_\odot$/yr. The detailed physics of the mass-loss process, the constituents of dust-seed particles, and the distribution of many species all remain poorly known. Unbiased wide bandwidth spectral line surveys are powerful tools to address these issues.

Observations of a broad suite of lines give us a comprehensive view of the basic chemical processes and reaction rates occurring as the wind cools and the elements combine to form the material that pervades the interstellar medium. Wide frequency coverage allows detection of several transitions from the same molecule, which allows for unambiguous identification, as well as determination of physical conditions. Examples of newly identified lines in space resulting from SMA surveys include the first detection of rotational transitions in vibrationally excited states in CO (Patel et al., 2009), C_4H (Cooksy et al., 2015), and, in concert with new laboratory measurements, SiCSi, a key species in the formation of dust grains (Cernicharo et al., 2015).

Figure 8 shows a 64 GHz wide integrated spectrum of the expanding envelope of the extreme carbon star IRC +10216 that was imaged by the SMA (Patel et al., 2011). The spatial extent of the emission indicates the radial distance in the flow where molecules form first. A total of 442 spectral lines were detected in this survey, more than 200 for the first time (and more than 100 remain are unassigned). A substantial new population of narrow lines were detected for the first time with an expansion velocity only 30% of the terminal velocity, all concentrated within $1''$ of the star, probing the region of wind acceleration and dust formation. While this spectral line survey required 13×8 hour tracks with the SMA, an equivalent survey could be conducted in a single track with the wSMA (with the additional benefit of improved and uniform calibration). With the wSMA, it will be possible to make the observations needed to compare spectral lines imaged from a large sample of evolved stars, with a range of chemistries (e.g. Oxygen rich vs. Carbon rich), rather than relying on conclusions drawn from a single target.

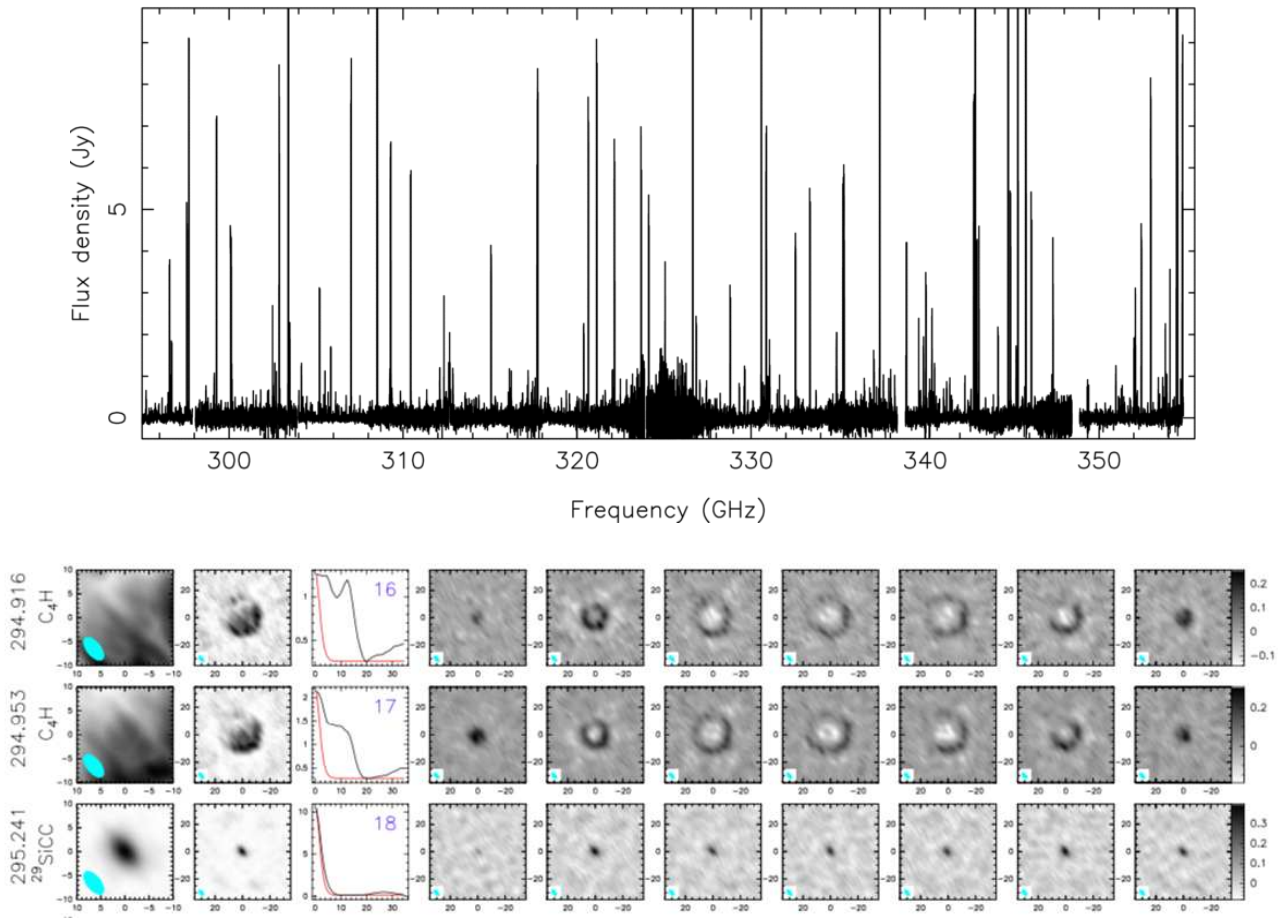

Figure 8: (upper) *The integrated 64 GHz spectrum of the evolved star IRC+10216 from the SMA line survey of Patel et al. (2011), with 442 lines detected.* (lower) *Sample images showing the emission line structure for a few lines at the low frequency end of the survey, including integrated intensity, radial profile, and velocity resolved channel maps. Note the ring -like distribution of C_4H compared to the compact and strongly centrally peaked distribution of SiCC; this butadinyl molecule is created in the outer part of the envelope where chemistry is influenced by the interstellar radiation field.*

4.1.5 Planetary Atmospheres

Planetary spectroscopy presents some of the most challenging observations that the SMA performs. At one extreme, measurement of spectral features from the upper atmospheres of Mars, Venus, Titan, and Io, where pressures are low, requires high spectral resolution, of order 100–200 kHz, in order to resolve the thermal line emission and to measure winds from Doppler shifts. The latter typically needs sensitivity down to 10 m s^{-1} (10 kHz at 300 GHz), which is only possible through line fitting over multiple channels. At the same time, broad bandwidths are often of interest: for example on Titan and Io, there are many species detectable covering a wide range of frequencies in the 230 and 345 GHz atmospheric windows. Figure 9 shows 36 GHz of the spectrum pieced together from more than 100 short and narrow band observations from the SMA archive resulting in highly non-uniform noise. This compilation resulted in the first reported detections at these wavelengths of DCN, CH_3C_2H, and vibrationally excited HC_3N and CH_3CN (Gurwell et al., 2012). The wSMA would survey more of the spectrum, to greater uniform depth, in a single track. Note that the linewidths of some species on Titan like CO and HCN exceed 1 GHz, and thus a broad bandwidth coupled with stable passband characteristics is vital for precise line analysis.

At the other extreme, some lines from the gas giants (Jupiter, Saturn), ice giants (Uranus, Nep-

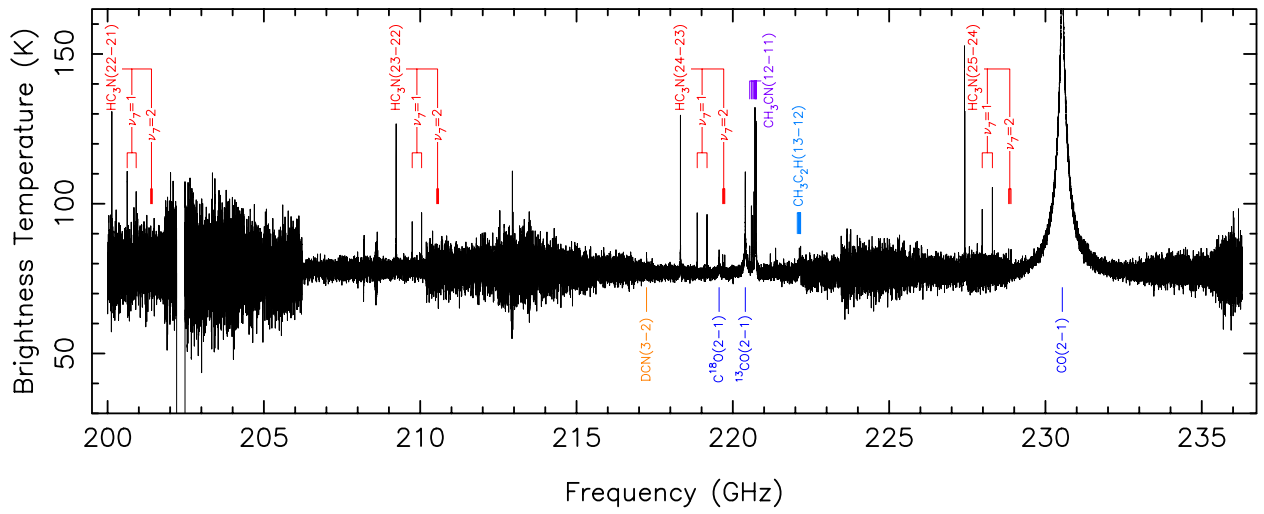

Figure 9: *A serendipitous 36 GHz line survey of Titan, obtained by piecing together more than 100 short, narrow band, archival observations (Gurwell et al., 2012). Each observation was calibrated, aligned, and smoothed to a common spectral resolution, and scaled to a common source reference diameter.*

tune), and Venus are extremely wide due to pressure broadening. The CO(2-1) and (3-2) transitions on Neptune span up to 20 GHz, and PH3(1-0) at 267 GHz spans 30 GHz on Jupiter and Saturn. These are deep transitions, but radiative and chemical modeling of the spectra of these planets suggest there are other spectral lines, similarly broad but shallow, awaiting detection. Both Uranus and Neptune are expected to show H_2S and/or PH_3 lines spanning 10–20 GHz in width, but with depths just a few percent of the continuum. Similarly, Venus may exhibit lines of sulfur bearing species that are many GHz wide but also shallow. Such lines are difficult to detect without a very broadband wavelength coverage, along with system stability that enables precise calibration of the broadband spectrum. The wSMA will be exceptional in this regard. The simultaneous end to end coverage of up to 40 GHz is well matched to the broad line characteristics of the gas and ice giants. Morever, the combination of broad spectral coverage with high spectral resolution, sufficient to resolve even thermal lines, is ideal for detailed line surveys of Titan and Io.

4.2 Time Domain Studies

The transient and variable Universe provides critical information on a wide range of astrophysical sources and problems. At submillimeter wavelengths, time domain studies are essential for understanding high energy sources such as active galactic nuclei, black hole binaries, gamma-ray bursts, novae, and supernovae, as well as young stellar objects. Many of these sources are very bright and readily detectable with the SMA. Others are faint, fading, or entirely unknown, and rapid result sharing based on quick look analysis is critically important for follow-up (detection or limits, disseminated by ATel or other relevant networks). This work often requires very fast response times and high cadence monitoring that are operationally or programmatically difficult to achieve with ALMA. A wide instantaneous bandwidth can be particularly advantageous for observing phenomena that exhibit rapid time variability, from timescales of minutes to hours to years. Beyond the raw continuum sensitivity, broad spectral coverage provides a long lever in frequency, e.g. to measure Farady rotation, and additionally gives access to many molecular species and transitions at once. The wSMA will be well positioned for successful exploitation of time domain science.

4.2.1 Polarized emission from SgrA*

In the Galactic Center, relativistic electrons in the magnetized plasma around the supermassive (4×10^6 $M_\odot$) black hole SgrA* emit polarized synchrotron radiation. On passing through the ionized accretion flow into the black hole, the angle of the polarization changes by an amount directly proportional to the product of the strength of the magnetic field and the electron density, and inversely proportional to the observing frequency squared (Faraday rotation). With some assumptions about the structure of the accretion flow and the relationship between the magnetic field strength and the density, the difference in the polarization angle measured at two different frequencies yields the accretion rate into the black hole. At long millimeter and radio wavelengths, the presence of an ionized screen depolarizes the signal, leaving the submillimeter as an important window into the accretion physics of this black hole. The SMA made the first reliable measurement of the SgrA* Faraday rotation $(-5.6 \pm 0.7) \times 10^5$ rad m^2, which provided critical constraints on the accretion rate, $2 - 200 \times 10^{-9}$ $M_\odot$ yr^{-1} (Marrone et al., 2007), depending in detail on the geometry and (dis)order of the magnetic field. Previously, Faraday rotation had been measured by comparing observations at different frequencies at different times. However, because the emission from SgrA* is time variable in both intensity and polarization, the results of these earlier observations were highly uncertain. Moreover, high angular resolution has proven critical to isolate SgrA* from its extended (and also polarized) surroundings.

One of the mysteries of the SgrA* black hole is why it is normally so quiet, particularly in high energy radiation. It may have a very low accretion rate, or alternatively, the accretion flow may be cooled by advection rather than radiation. In these advective accretion flows (ADAFs) most of the energy released by the deceleration of the accretion flow actually disappears into the black hole leaving relatively little observable radiation. We hope to measure the accretion rate accurately enough to test the ADAF hypothesis.

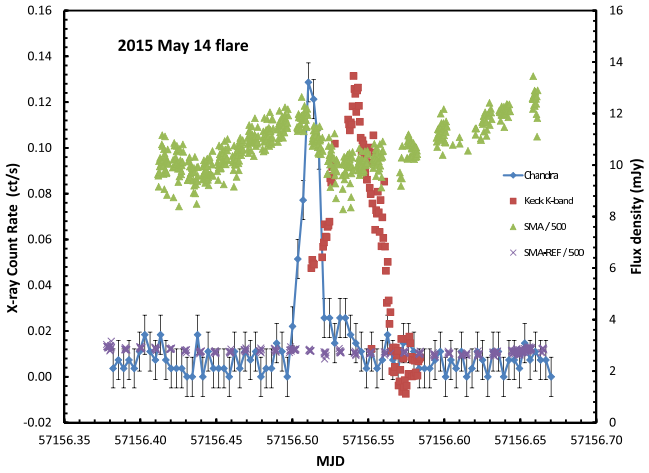

Figure 10: *Light-curves of SgrA* in the submillimeter (SMA), infrared (Keck) and X-ray (Chandra), showing a flare with a timescale of order an hour (Marrone et al., 2016). The wSMA will provide sufficient continuum sensitivity to detect such flares easily and to measure changes in polarization during the flare events.*

Another mystery is the flares observed at wavelengths from the X–ray to the radio. What causes them? Are they periodic? Are events at different wavelengths correlated? SgrA* is a bright object in the submillimeter, typically a few Jy, and 5–10% polarized. Figure 10 shows one flare with a timescale of about an hour that was seen with both the SMA in the submillimeter and Keck telescope in the near-infrared (Marrone et al., 2016). The wSMA would be able to monitor the variations in Faraday rotation in SgrA*, and hence variations in the accretion rate, on time scales as short as the flares. For example, if the flaring is caused by a jet or outburst unrelated to the accretion, then the Faraday rotation should remain constant during the flare. If the flare is related to the accretion flow itself through magnetic reconnection or an increase in the accretion rate, then the Faraday rotation should change with the flare. The wSMA could conceivably devote weeks or months to monitoring the activity of SgrA*, to characterize the variability of its submillimeter emission.

An analysis of archival SMA data on SgrA* as well as nearby low luminosity active galactic nuclei M81 and M87, has revealed a linear relationship between the characteristic variability time scale and the black hole mass (Bower et al., 2015). This relationship demonstrates that the emission in

these systems originates from within $\sim$ 10 Schwarzschild radii of the black hole. Blazars and radio galaxies do not follow the same relationship. Ongoing monitoring of other low luminosity AGN will expand the sample over which the relationship holds. Monitoring of all these systems is critical for interpreting Very Long Baseline observations, which require detailed spectral modeling, as well as for providing triggers for rapid response in the case of flares (see §5.1).

4.2.2 Comets

The comets that cross our Solar System are messengers from the past, bringing with them original, pristine, material from the epoch of planet formation. Minimally processed material is released in jets outgassing from the interior through cracks in the comet surface. Interferometry provides a means of imaging and isolating the jet emission within the larger coma that is dominated by outgassing from the comet crust. The left panel of Figure 11 shows a simulation of the submillimeter line intensities expected in the gaseous jet emission and from the extended coma from the comet's surface, assuming different chemical abundance models for each. In previous observations of the Jupiter family comet 17P/Holmes, observations over multiple days detected many molecular species, including CO, CS, HCN, H_2S, H_2CO, and CH_3OH (Qi et al., 2015). Howevever, the asymmetric jet emission changes on timescales of the comet rotation period (typically several hours), and the bandwidth was sufficient to observe only two lines of interest simultaneously, e.g. HCN 4–3 and CO 3–2, making comparisons difficult. The much wider instantaneous spectral coverage of the wSMA is advantageous in allowing comparative observations of many lines simultaneously, all at sub-km s^{-1} spectral resolution to clearly separate jet from coma.

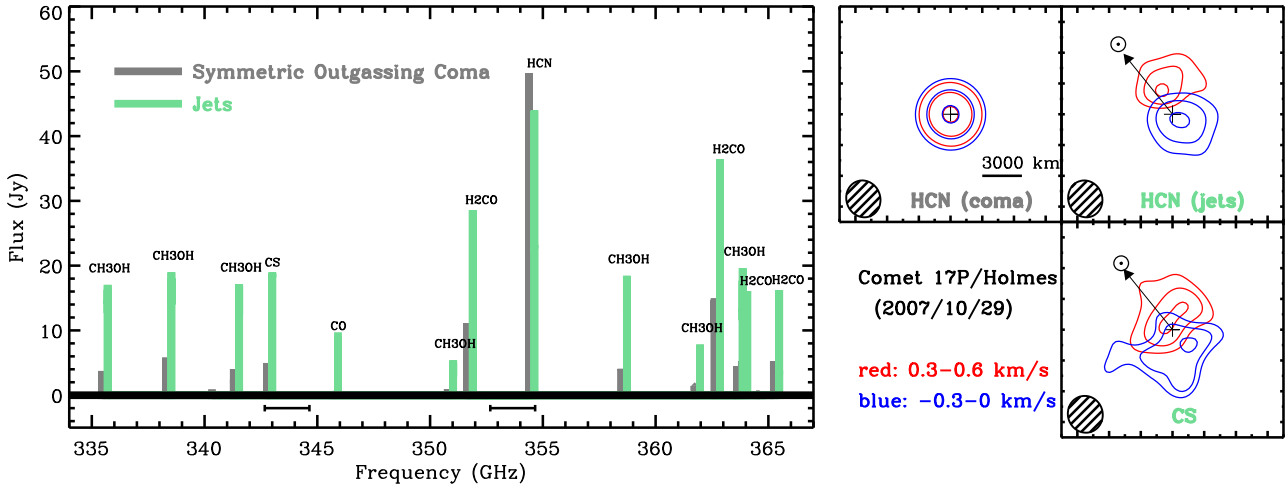

Figure 11: *(left) Simulation of molecular emission from a comet, showing a suite of spectral lines in the 345 GHz band that the wSMA could observe simultaneously at high spectral resolution to probe the abundances of jet and coma material. (right) SMA images of HCN and CS emission from comet P17/Holmes obtained simultaneously, showing blue- and red-shifted emission from a jet, and the extended coma.*

Comet observations seek to derive a chemical inventory of the pristine material from the emission in the submillimeter. One key question to be addressed concerns the origin of the comets. A working model posits two comet families: (1) the long period comets, formed in the giant planet zone and scattered into the Oort cloud by gravitational interactions, and (2) the short period or ecliptic comets, formed further out in the Kuiper Belt region. So far, spectroscopy does not yield a clear chemical distinction between the two. It is not known whether this results from a confusion of processed with pristine material, whether there was little chemical differentiation in the early Solar System, or whether this supports an alternative model. For example, it is possible that all the comets formed

in the same region and were scattered during a period of instability, e.g. in the Nice model, when the orbits of Jupiter and Saturn evolved through a 2:1 resonance.

4.2.3 Gamma Ray Bursts

Gamma-ray Bursts (GRBs) are some of the most powerful explosions in the universe and are observationally characterized by intense flashes at high energies (prompt emission) and long-lived afterglows from the X-ray to radio. Broad frequency coverage is essential to fully characterize the energetics. The radiation is occasionally extremely bright and can be observed with telescopes of modest aperture. GRBs have a bimodal distribution of durations, and the spectral hardness of prompt emission indicates distinct progenitor physics for "long-soft" and "short-hard" GRBs. The long GRBs occur in star-forming galaxies and are associated with the deaths of massive stars; these present a unique and powerful means to see the explosions of first generation stars. The short GRBs result from mergers of compact objects; these are plausible sources of gravitational waves. High cadence multi-band monitoring observations are needed to probe the explosion physics. The submillimeter is especially important for tracking the reverse shock emission associated with both types of GRBs. These events peak earlier and with higher flux densities in the submillimeter than in the radio.

In the standard relativistic fireball model for GRBs, a reverse shock propagates into the ejecta and radiates at long wavelengths by a synchrotron process in an early afterglow phase. Detecting this brief reverse shock emission and measuring its magnitude can provide constraints on important parameters of the GRB ejecta, such as its initial Lorentz factor and magnetization. While early time optical observations for GRBs have yielded no evidence of reverse shock emission in most cases, a possible reason for these nondetections is that the typical synchrotron frequency falls well below the optical band. The wSMA has the potential to search for reverse shock emission in the submillimeter. Very rapid response is required– 1 to 10 minutes from the GRB trigger. The SMA observations of GRB120326A (Urata et al., 2014) provide a benchmark for the importance of these wavelengths for understanding the afterglow emission. Figure 12 shows the spectral energy distribution at 6.4×10^4 seconds after the burst, with the SMA measurement anchoring the model fit to the reverse shock. For sufficiently bright GRBs (e.g. GRB151027A and GRB160623A detected by the SMA), polarization measurements can provide additional information on the emission mechanism and associated magnetic fields.

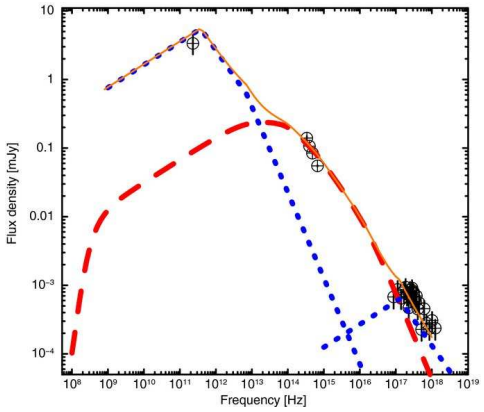

Figure 12: *The spectral energy distribution of GRB120326A,* 6.4×10^4 *seconds after the burst (Urata et al., 2014). The red dashed line shows the forward shock synchrotron model spectrum using parameters that match the light curve. The blue dotted lines show the reverse shock synchrotron radiation and its self-inverse Compton component calculated based on Kobayashi et al. (2007) using the observed values and model function for the forward shock component.*

Because GRBs have such high luminosities, events at the reionization epoch ($z \sim 8$) have been seen in the optical, and detection at higher redshifts is possible. Inoue et al. (2007) showed the reverse shock component of GRBs at $z = 15$ in the 300 GHz band is substantially brighter than 1 mJy, readily detectable with the upgraded SMA. Simulations of light curves at $z = 10, 15$, and 30 based on (Kobayashi, 2000; Kobayashi et al., 2007) show that the wSMA can detect GRBS at these redshifts, assuming rapid response and dense monitoring. Initial detections at early times will provide opportunities to conduct follow-up using ALMA and the largest optical telescopes. Since follow-up on these large telescopes is possible for only a limited number of events, target selection based on wSMA observations will be critical.

For short GRBs, the compact object merger model has been tested with host galaxy properties,

redshift distributions, and burst locations within the hosts. But these studies provide galactic-scale properties only, and the explosion physical parameters such as energetic and cirumburst density remain unconstrained. Like long GRBs, multi-frequency analysis of afterglow light curves and spectra are needed to improve understanding. So far, this hasn't been possible in the submillimeter. In the 2020s, a dedicated GRB satellite mission SVOM will become operational, and, unlike the current random pointings from Swift, the GRB detectors will observe anti-sun directions that enable rapid follow-up with ground-based instruments and continuous long-term monitoring (Wei et al., 2016). In addition, because short GRBs share a common compact object merger model with gravitational wave sources, this is a timely topic as precise timing from several gravitational wave instruments will provide position information to search for electromagnetic counterparts. The sensitivity of these gravitational wave detectors is expected to reach the signal from binary neutron stars out to about 100 Mpc.

To take full advantage in this science area, the wSMA will require a mode that provides for very rapid response time, ideally within a minute, perhaps using automatic responses to satellite triggers.

4.3 Magnetic Field Imaging and Star Formation

Observations of magnetic field structures address a fundamental unknown in star formation. Magnetic forces are easily comparable in magnitude to other forces, and some theories assert that the formation of molecular clouds and their subsequent contraction to form stars is controlled entirely by magnetic forces. This hypothesis has been neither verified nor disproven because of a lack of evidence, and because of the challenging nature of the observations required. Magnetic fields are themselves invisible, but their structure in the interstellar medium is made evident in the pattern of polarized continuum emission emitted by dust grains that align with the field. The SMA has made numerous studies of polarized millimeter and submillimeter dust continuum emission to map the magnetic fields in accretion flows around low-mass protostars (Girart et al., 2006; Rao et al., 2009) and high-mass protostars (Girart et al., 2009; Zhang et al., 2014), and in large-scale molecular clouds (Li & Henning, 2011). Figure 13 shows an example, the SMA image of the magnetic field structure in the accretion flow onto the low-mass protostellar system NGC1333 IRAS4A, which is organized into a classic hour-glass pattern, pinched in by gravitational collapse. Detailed analysis of these SMA data shows that the magnetic field morphology threading the core matches well the theoretical predictions from magnetohydrodynamic models of protostellar collapse (Gonçalves et al., 2008). For regions of high-mass star formation, dust polarization observations with the SMA have shown patterns that range from ordered hour-glass configurations to more chaotic distributions. Comparisons of these SMA results at < 0.1 pc scales with single dish observations at > 1.0 pc scales suggest that the magnetic fields play an important role in the collapse and fragmentation of massive clumps and the formation of dense cores (Zhang et al., 2014).

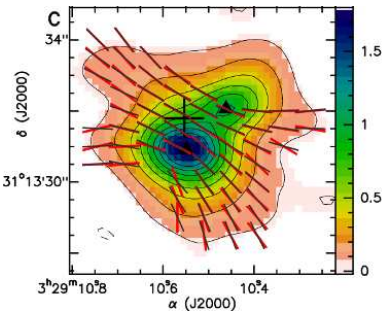

Figure 13: *SMA observations of polarized 870 μm dust continuum emission from NGC 1333 IRAS 4A provided the first textbook example of an hourglass-shaped magnetic field (red bars) in a low mass protostellar system (Girart et al., 2006). The color image shows the dust emission from the dense molecular core that surrounds two still-forming Sun-like stars. Gravity pulls the gas and dust of this cloud clump inward and warps the magnetic field in the process.*

For the wSMA, the improved continuum sensitivity resulting from increased bandwidth allows for (1) imaging of many more and fainter systems to build large samples, (2) imaging select systems at higher angular resolution, and (3) imaging wide field of view mosaics to connect magnetic features across the rnage of scales from clouds to cores to disks. The wSMA will increase the number of

clouds with fully mapped magnetic fields from a handful to a significant number, finally enabling stringent observational tests of these competing theories. While the high sensitivity and high angular resolution of the ALMA 12 meter antenna array will make it the facility of choice for dust polarization observations of small scale structures such as accretion disks, the wSMA, with its wider field of view, can be employed to advantage for observations of magnetic fields at larger scales and at modest resolution. For example, SMA observations showed that the magnetic field direction within giant molecular clouds in the spiral arms of the galaxy M33 is aligned with the larger galactic-scale field (Li & Henning, 2011). This study suggests that formation of large-scale clouds is a magnetic phenomenon. But, similar studies must be done in many more galaxies to understand the generality of this result, and its applicability in different environments.

To fully characterize the role of magnetic fields in Galactic regions of star formation will require sufficiently extensive dust polarization observations to span the full range of scales from entire molecular clouds down to the accretion disks surrounding protostars. In the next few years, the POL-2 instrument on the JCMT is expected to produce a treasure trove of wide-field 850 μm dust emission polarization maps of star-forming clouds, dense cores and filaments, at 14$''$ resolution. Complementary images with the wSMA at an order of magnitude higher angular resolution will be critical to connect the larger scale features visible in these single dish surveys to the smaller scales of individual protostellar envelopes, and ultimately to the subarcsecond scales of embedded accretion disks expected to be revealed by ALMA. The wSMA is particularly well suited to large scale magnetic field mapping of star forming regions, and will outperform the ACA for this application. Already, tests with the SMA of multiple pointing polarization observations show agreement of better than 1% in polarization angle in overlapping regions, as well as very low systematic uncertainties in leakage terms on- and off-axis, giving confidence in this observing mode. Observations of dozens of star forming regions will enable determination of the statistics of magnetic field strengths using the Chandrasekhar-Fermi method, on all relevant scales. These high resolution images will show directly the field morphology, without need to appeal to any specific model. Comparison of wSMA, JCMT and ALMA dust polarization data will enable magnetic field features to be related to molecular line images and to changes in gravitational and rotational energy within key structures.

5 Additional Science Modes

5.1 VLBI: The Event Horizon Telescope

Scientific interest in submillimeter Very Long Baseline Interferometry (VLBI) is now driven largely by the quest to directly observe the immediate environments of black holes with resolution comparable to the scale of the event horizon. Data from an Earth-sized "Event Horizon Telescope" (EHT) holds the promise to probe key issues in black hole physics, including the validity of the event horizon predicted by General Relativity, as well fundamental astrophysical processes of disk accretion and jet launching. The SMA has already played a key role, by virtue of early deployment of enabling hardware and the strategic geographic location of Maunakea at near-equatorial latitude in the mid-Pacific. Three station millimeter VLBI observations including Maunakea obtained the first detections of emission at Schwarzschild radius scales in SgrA* and M87, two of the most promising black hole targets for more detailed study (Doeleman et al., 2008, 2012). Recently, millimeter VLBI polarization observations have revealed highly ordered magnetic field structure and time variability at these scales (Johnson et al., 2015).

Advances in receiver capabilities, digital signal processing for wide bandwidths, and the development of new millimeter and submillimeter VLBI stations, all point to prospects for revolutionary observations over the next decade. In particular, the fully phased ALMA for VLBI, with collecting

area equivalent to an 80 meter single dish, offers a major boost in sensitivity. The EHT is on track to realize the goal of recording the full bandwidth of the ALMA system (8 GHz $\times$ 2 polarizations) at all available stations for observations in 2017. At the SMA, the SWARM correlator has been designed from the ground up for VLBI operations. The SMA provides the only long east-west baselines in the EHT, as well as a simultaneous reference for flux and polarization. The SMA will continue to provide important long baselines to the EHT in the push to observations at 345 GHz to achieve higher angular resolution, as one of the few stations with reliable weather for operations at these high frequencies. Since it will always be difficult to make observations at all stations, the SMA offers an important opportunity for VLBI with a subset of the EHT for extremely valuable (non-imaging) observations. Finally, the capability to observe simultaneously at 230 and 345 GHz could prove to be an exciting development for future VLBI experiments, e.g. together with ALMA operating in two subarrays. The SMA is fully committed to participation in EHT observations.

5.2 Opportunities: Higher Frequencies, Multi-Beam Receivers, and More

The wSMA design explicitly incorporates an open receiver port that can be instrumented in a flexible way to address compelling science goals, or to pursue technical innovations. Such receivers could be developed in the context of new external collaborations or limited partnerships. This provision will allow the SMA to continue its role as a major pathfinder in submillimeter astronomy and instrumentation.

As a science driven example, we consider the possibility of a new receiver set to target the 492 GHz fine-structure line of neutral atomic carbon (CI). Carbon is the fourth most abundant element and an important species in the chemistry and energy balance of interstellar gas. Unlike other common elements, all of the key phases of carbon are accessible to observation, including neutral atomic carbon (CI), ionized carbon (CII), molecular carbon (CO), and carbon in dust grains. In particular, *Herschel* and now *SOFIA* provide an inventory of CII observations, and while supporting CO data is easy to come by, the complementary CI data are challenging to obtain, especially at high angular resolution. These data are especially important for understanding photodisociation regions, where starlight interacts with dense gas in environments as diverse as starburst galaxies and the surfaces of protoplanetary disks. The far ultraviolet radiation ejects electrons from dust grains that collide with and heat the gas. Observations of the full suite of carbon phases will test chemical and thermal models of these regions, which predict that the CI lines trace the transition between CII and CO. While such observations are possible with ALMA, the time available for the requisite observations (in ALMA band 8) is extremely limited, especially in light of competition from all higher frequency bands. A dedicated receiver set on the wSMA would enable a thorough study.

As a technology driven example, we consider the possible development of multi-beam heterodyne receivers for submillimeter interferometry. This would be particularly welcome for the higher frequency bands where observing is limited to a small fraction of time under the best weather conditions. While a few submillimeter focal plane arrays have been deployed on single dish telescopes, this technique has not been established on interferometers for wide field mapping at high angular resolution. The combination of spatial and spectral multiplexing enabled by multi-beam receivers offers considerable advantages for pursuing a variety of science goals. The wSMA could much more easily incorporate array receivers than a large array like ALMA on account of its modest scale. The deployment of modest-sized multi-beam receiver sets has the potential to make the wSMA the most efficient facility for wide-field millimeter/submillimeter imaging at high angular resolution. The future of the wSMA in the longer term, beyond the time frame considered in this whitepaper, will depend on the development of new technologies like this, together with affordable strategies for implementation and operations.

Acknowledgements

The authors wish to recognize and acknowledge the very significant cultural role and reverence that the summit of Maunakea has always had within the indigenous Hawaiian community. We are most fortunate to have the opportunity to conduct observations from this mountain.

6 References

Andrews, S. M., Wilner, D. J., Hughes, A. M., Qi, C., & Dullemond, C. P. 2009, ApJ, 700, 1502

Andrews, S. M., Wilner, D. J., Espaillat, C., et al. 2011, ApJ, 732, 42

Bower, G. C., Dexter, J., Markoff, S., et al. 2015, ApJ, 811, L6

Bradford, C. M., Bolatto, A. D., Maloney, P. R., et al. 2011, ApJ, 741, L37

Breysse, P. C., Kovetz, E. D., & Kamionkowski, M. 2015, MNRAS, 452, 3408

Bussmann, R. S., Pérez-Fournon, I., Amber, S., et al. 2013, ApJ, 779, 25

Cañameras, R., Nesvadba, N. P. H., Guery, D., et al. 2015, A&A, 581, A105

Cernicharo, J., McCarthy, M. C., Gottlieb, C. A., et al. 2015, ApJ, 806, L3

Cooksy, A. L., Gottlieb, C. A., Killian, T. C., et al. 2015, ApJS, 216, 30

Cyganowski, C. J., Brogan, C. L., Hunter, T. R., et al. 2014, ApJ, 796, L2

Doeleman, S. S., Weintroub, J., Rogers, A. E. E., et al. 2008, Nature, 455, 78

Doeleman, S. S., Fish, V. L., Schenck, D. E., et al. 2012, Science, 338, 355

Dowell, C. D., Conley, A., Glenn, J., et al. 2014, ApJ, 780, 75

Fazio, G., Bergin, E. Carilli, C., Ho, P., Marrone, D., Menten, K., Paine, S., Shu. F., Stacey, G. 2010, *Report of the Committee on the Future of the SMA*, https://www.cfa.harvard.edu/sma/meetings/Futures/2009

Girart, J. M., Rao, R., & Marrone, D. P. 2006, Science, 313, 812

Girart, J. M., Beltrán, M. T., Zhang, Q., Rao, R., & Estalella, R. 2009, Science, 324, 1408

Gonçalves, J., Galli, D., & Girart, J. M. 2008, A&A, 490, L39

Gurwell, M. A., Butler, B. J., & Moullet, A. 2012, AAS/Division for Planetary Sciences Meeting Abstracts, 44, #312.12

Harris, A., Gammie, C., Guelin, M., Menten, K., Plambeck, R., Turner, J. 2014 *Submillimeter Array Advisory Committee Report*, https://www.cfa.harvard.edu/sma/meetings/Advisory/2014

Inoue, S., Omukai, K., & Ciardi, B. 2007, MNRAS, 380, 1715

Johnson, M. D., Fish, V. L., Doeleman, S. S., et al. 2015, Science, 350, 1242

Jørgensen, J. K., Bourke, T. L., Nguyen Luong, Q., & Takakuwa, S. 2011, A&A, 534, A100

Kamiński, T., Gottlieb, C. A., Young, K. H., Menten, K. M., & Patel, N. A. 2013, ApJS, 209, 38

Keating, G. K., Bower, G. C., Marrone, D. P., et al. 2015, ApJ, 814, 140

Kobayashi, S. 2000, ApJ, 545, 807

Kobayashi, S., Zhang, B., Mészáros, P., & Burrows, D. 2007, ApJ, 655, 391

Li, H.-B., & Henning, T. 2011, Nature, 479, 499

Lidz, A., & Taylor, J. 2016, ApJ, 825, 143

Maiolino, R., Carniani, S., Fontana, A., et al. 2015, MNRAS, 452, 54

Marrone, D. P., Moran, J. M., Zhao, J.-H., & Rao, R. 2007, ApJ, 654, L57

Marrone, D. P., 2016 et al. in preparation

Martín, S., Krips, M., Martín-Pintado, J., et al. 2011, A&A, 527, A36

Narayanan, D., & Krumholz, M. 2016, arXiv:1601.05803

Negrello, M., Hopwood, R., De Zotti, G., et al. 2010, Science, 330, 800

Parsons, A., Werthimer, D., Backer, D., et al. 2009, astro2010: The Astronomy and Astrophysics Decadal Survey, 2010, 21

Patel, N. A., Young, K. H., Brünken, S., et al. 2009, ApJ, 691, L55

Patel, N. A., Young, K. H., Gottlieb, C. A., et al. 2011, ApJS, 193, 17

Primani, R. et al. 2016, JAI, submitted
Qi, C., Hogerheijde, M. R., Jewitt, D., Gurwell, M. A., Wilner, D. J. 2015, ApJ, 799, 110
Rao, R., Girart, J. M., Marrone, D. P., Lai, S.-P., & Schnee, S. 2009, ApJ, 707, 921
Rawle, T. D., Egami, E., Bussmann, R. S., et al. 2014, ApJ, 783, 59
Riechers, D. A., Bradford, C. M., Clements, D. L., et al. 2013, Nature, 496, 329
Sakamoto, K., Wang, J., Wiedner, M. C., et al. 2008, ApJ, 684, 957
Sakamoto, K., Aalto, S., Costagliola, F., et al. 2013, ApJ, 764, 42
Smit, R., Bouwens, R. J., Franx, M., et al. 2012, ApJ, 756, 14
Tong, C.E., Blundell, R., Megerian, K.G., Stern, J.A., Pan, S.–K., Popieszalski, M. 2005, IEEE Trans. Appl. Supercond., 15, 490
Urata, Y., Huang, K., Takahashi, S., et al. 2014, ApJ, 789, 146
Wang, W.-H., Cowie, L. L., Barger, A. J., & Williams, J. P. 2011, ApJ, 726, L18
Wei, J., Cordier, B., Antier, S., et al. 2016, arXiv:1610.06892
Wolfire, M. G., Hollenbach, D., & McKee, C. F. 2010, ApJ, 716, 1191
Younger, J. D., Fazio, G. G., Huang, J.-S., et al. 2007, ApJ, 671, 1531
Younger, J. D., Fazio, G. G., Huang, J.-S., et al. 2009, ApJ, 704, 803
Zhang, Q., Qiu, K., Girart, J. M., et al. 2014, ApJ, 792, 116